Fundamentals of Detector Physics and Measurements Lab - IV

Carl Bromberg
Michigan State University
Dan Green
Fermilab

June 18-22, 2012

Outline

- Lecture I
  - Constants, atoms, cross sections
  - Photoelectric, TOF
  - PMT, SiPM Scint, Cerenkov
- Lecture II
  - Collisions, cross sections
  - Multiple scattering, radiation length
  - dE/dx, MIP, Range
  - Critical Energy

Outline II

- Lecture III
  - B fields, trajectories
  - Quadrupoles, focal length
  - Drift and Diffusion
  - Pulse formation in unity gain and gas gain
- Lecture IV
  - Radiation NR, Thompson, Compton
  - Relativistic radiation
  - Bremm, Pair Production

Si Vertex and b decays

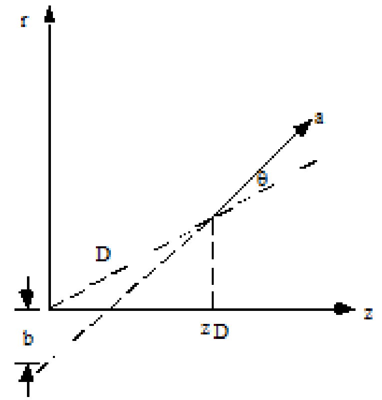

Geometry of a short-lived particle D decaying into a secondary track a with impact parameter b.

$$z_D \sim \gamma_D (c\tau)_D \sim D \qquad (9.1)$$
$$b \sim \theta z_D$$

$$D \to a + b$$
$$p_T^a \sim M_D / 2$$
$$p^a \sim p_D / 2$$

$$\theta \sim M_D / p_D \sim 1/\gamma_D$$
$$b \sim (c\tau)_D$$

HEP collider detectors have "vertex detectors" which serve to tag the production and decay of heavy flavors. The "impact parameter" b, is ~ the proper decay length of the parent. The spatial resolution should be << b.

$$\sigma^2 \equiv \left\langle \left(y - \langle y \rangle\right)^2 \right\rangle, \langle y \rangle = 0$$
$$= \left[\int y^2 dy / \int dy\right] -$$
$$\int_{-P/2}^{P/2} y^2 dy / \int dy$$
$$= P^2 / 12$$

b Tagging

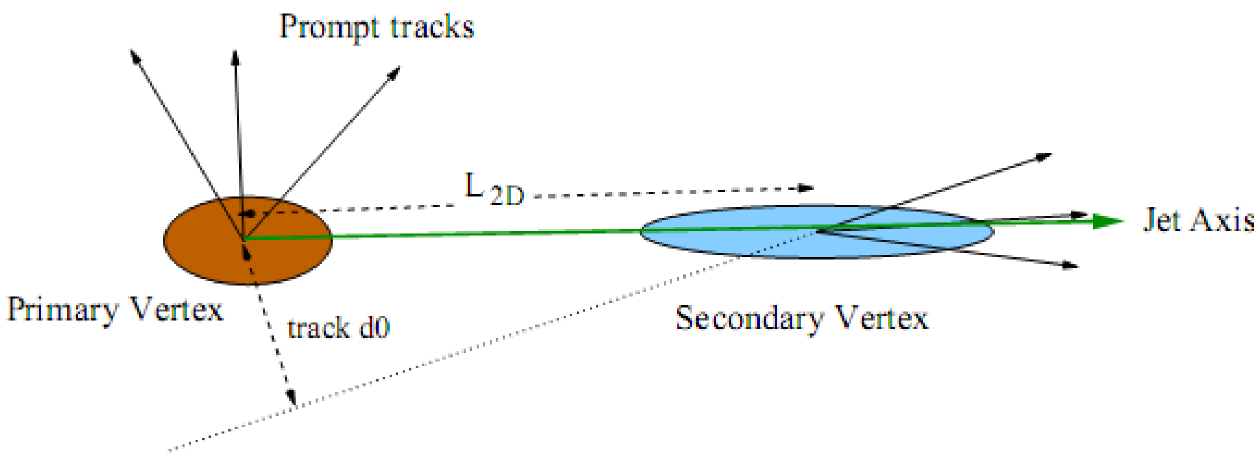

Figure 4: Displaced secondary vertex from decay of a long-lived particle. Tracks from the decay are not expected to point back to the primary vertex as prompt tracks do. Flavor tagging (b-tagging) algorithms are designed to identify tracks with significant impact parameter d_0 and a vertex with significant decay length L_{2D}.

Impact parameter, decay length and mass of tracks at the decay point are all possible tagging variables.

CMS 7 TeV – Heavy Flavor, (b)

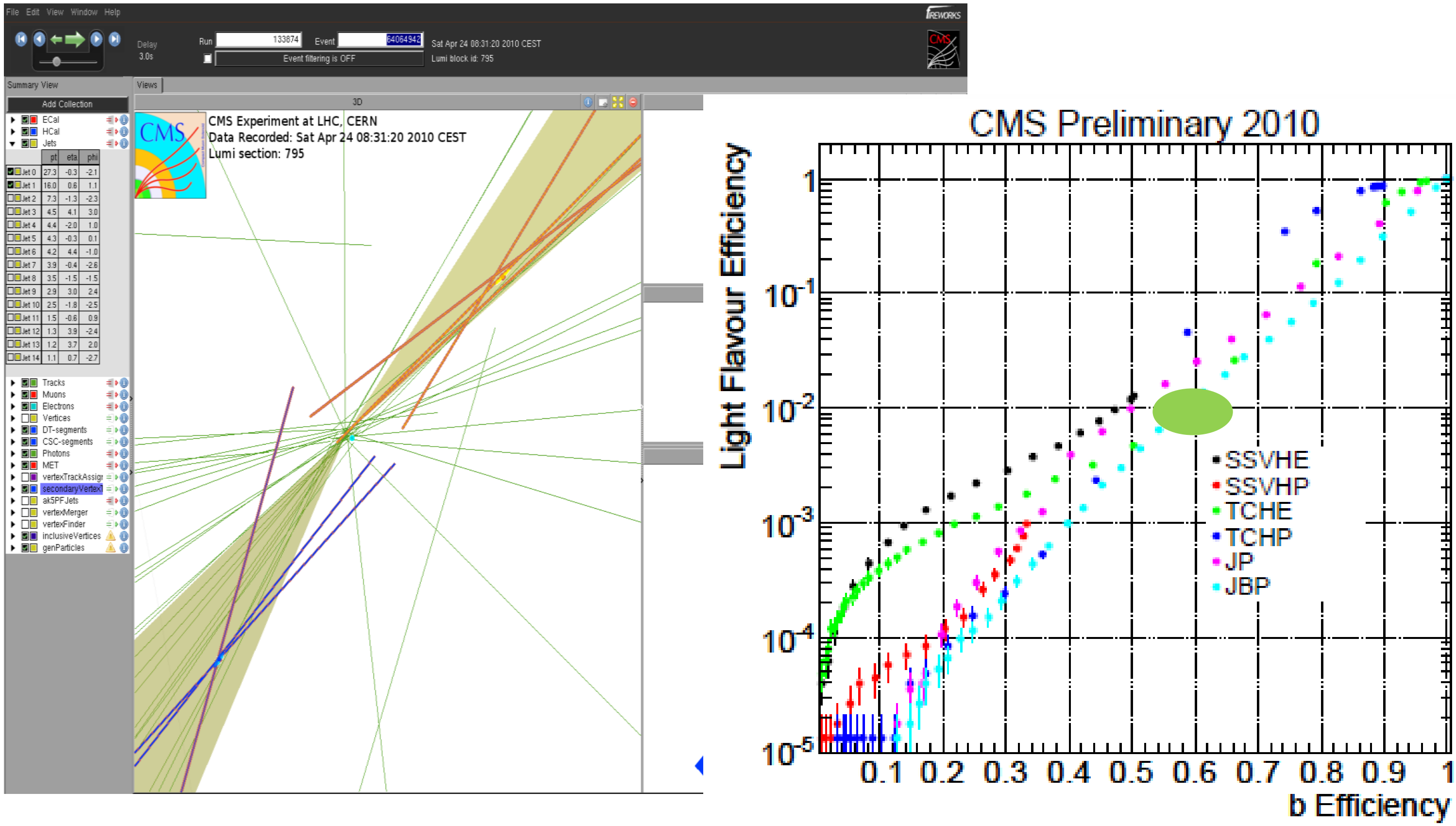

Note error ellipses on the primary and secondary vertices. Typical operating point is 60% efficient with a light flavor rejection of 100.

Intrinsic/Doped Si

$$n_{si} = \frac{N_o \rho}{A} \sim 5.01 \times 10^{22} / cm^3, n_i / n_{si} \sim 10^{-12}$$

$$n_i = p_i = 10^{11} / cm^3 \Big|_{T = 300 K^o}$$

$$\rho_i = 1 / q \mu n_i = 200 k\Omega cm$$

$$= 1 / \sigma_i$$

$$E_{pair} \sim 3.6\, eV$$

$$d \sim 300\, \mu m$$

$$q_s \sim q \left(\Delta E_{ion} / E_{pair} \right)$$

$$q_s \sim 5\, fC \sim 32{,}000\, q$$

Intrinsic charge is due to thermal excitation of a e-h pair. Since kT ~ 1/30 eV and Eg~ 3.6 eV this charge is very small and intrinsic Si has a high resistivity. Therefore very low levels of donor(n) and acceptor (p) states can determine the resistivity and the majority charge carriers

A typical detector has a MIP signal of ~ 5 fC or ~ 32 thousand e-h pairs in the VB-CB.

Si Energy Bands

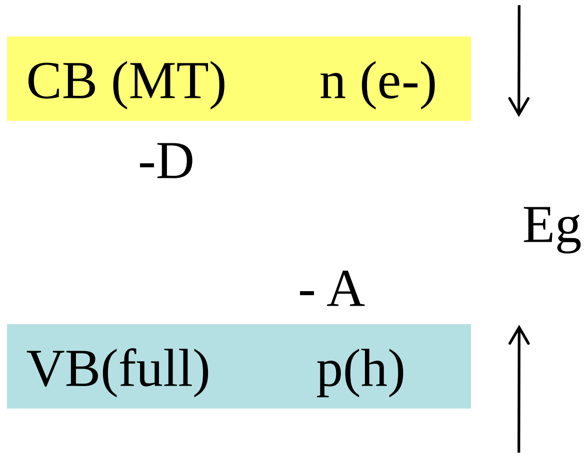

Excite e- to CB from donor states in gap, leave fixed + ions

Excite e- into acceptor states leaving mobile holes in VB. The – fixed states remain

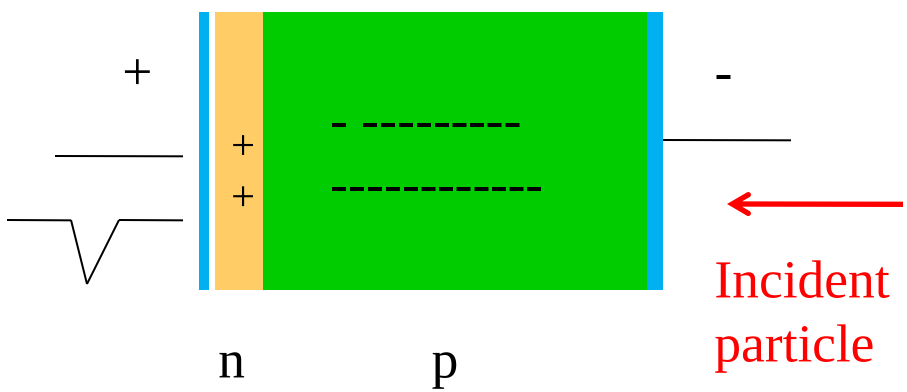

Si Diode

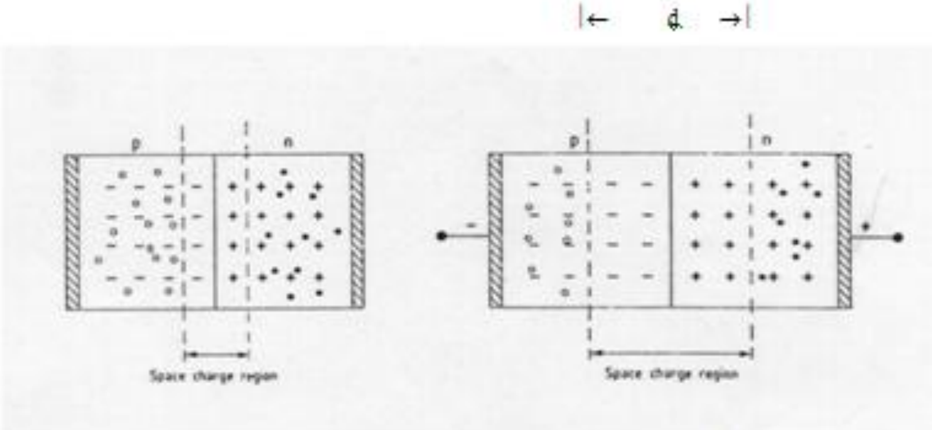

Schematic of a reverse biased p-n semiconductor diode showing the depletion region. (From Ref. 11, with permission.)

"Dope" Si with a small fraction of donor/acceptor sites which are still >> intrinsic conductivity. Form a diode from a sandwich of n and p type.

$$I(V) = I_o\left[e^{qV/kT} - 1\right]$$

$$R_F \equiv (dI/dV)^{-1} = \frac{kT}{qI} = 25\Omega\Big|_{300^oK,1mA}$$

Io = reverse current (minority carriers). V< 0 Forward bias, V > 0 (majority carriers)

Si Diode - II

$n_A A = n_D D$ Charge is conserved

$$\vec{\nabla} \cdot \vec{D} = \rho$$

$$\vec{\nabla} \cdot \vec{E} = [qn] / \underline{C} \;,\; \underline{C} \;\; or \;\; \varepsilon \; (CGS)$$

Applied voltage => depletion region. Charge swept to electrodes. Static charge remains, p type < 0, n type > 0.

$$E(x>0) = -qn_A(x-A)/\underline{C}$$

$$E(x<0) = qn_D(x+D)/\underline{C}$$

$$= q\left[\frac{n_A A}{D}\right](x+D)/\underline{C}$$

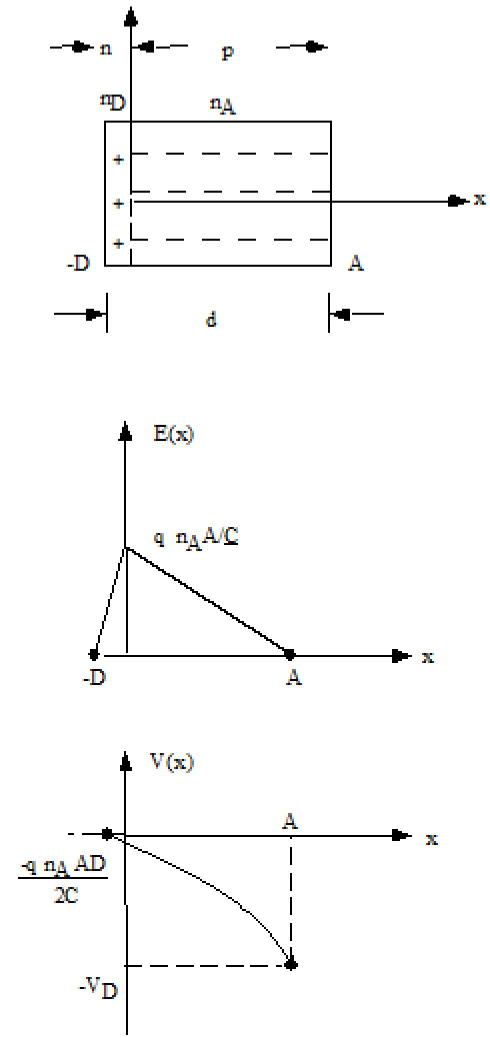

a) Geometry of a p-n junction. The static charge number density is n_D and n_A. The full depletion region is d = A +D ~A. b) Electric field for a p-n junction. c) Electric potential for a p-n junction.

Si Diode Fields - Depletion

$$\vec{E} = -\vec{\nabla} V$$ potentials

Derive V from E.

$$V(x<0) = -\frac{q\, n_A A (x+D)^2}{2D\underline{C}}$$

$$(V(x>0)+V_D) = \frac{q\, n_A (x-A)^2}{2\underline{C}}$$

d~A, fully depleted when all free carriers are swept to electrodes.

Just at depletion the electric field is 0 at the electrode location

$$V_D \sim q n_A d^2 / 2\underline{C}$$

$$V_D = [qp] d^2 / 2\underline{C}, \left(\frac{2\pi}{\varepsilon} [qp] d^2, MKS \right)$$

Si – Pulse Formation

Si is a unity gain device, so the treatment is as before.

$E(x) = -\left(\frac{2V_D}{d^2}\right)(x-d)$. For $V_D = 50V$ and $d = 300\mu m$ is $E(0) = 3kV/cm$ Just at depletion

$$dx = \mu E dt = -\mu\left(\frac{2V_D}{d^2}\right)(x-d)dt$$

E field is 0 at x=d, drift velocity

$$x(t) = d\left[1-e^{-t/\tau_D}\right],\ \tau_D = \underline{C}/\mu[qp],$$

$$x(0) = 0,\quad x(\infty) = d$$

Line ionization over distance d, t = arrival time at electrode

$$I(t) = dQ/dt = \mu q_s E^2/V_D,$$

$$= \frac{4\mu q_s V_D}{d^2} e^{-2t/\tau_D} = 2q_s/\tau_D\left[e^{-2t/\tau_D}\right]$$

Time to collect charge at depletion = distance/drift velocity @ x=0.

$$I(o) = 2q_s/\tau_D$$

$$I(\infty) = 0$$

$$\tau_D = \left[d^2/2V_D\mu\right]$$

$$= d/\left[\mu E(0)\right]$$

$q_s = 5fC$

$\tau_D \sim 7n\sec(20n\sec)$ e, h

$I(o) \sim q_s/\tau_D = 710nA(240nA)$

Si Pixels

MATRIX OF PADS ON SILICON WAFER, BUMP-BONDED TO READOUT ELECTRONICS:

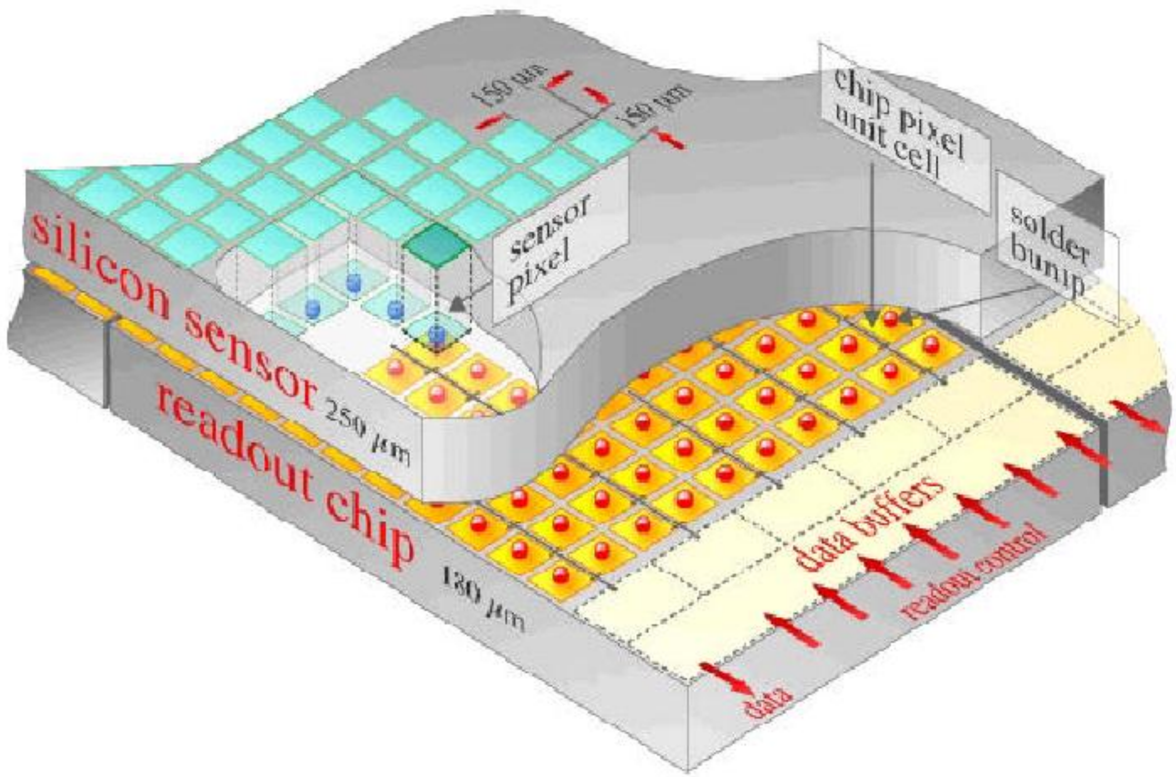

Present pixel generation = diode pixels bump bonded to readout chip.

3-d Silicon

3D-Introduction

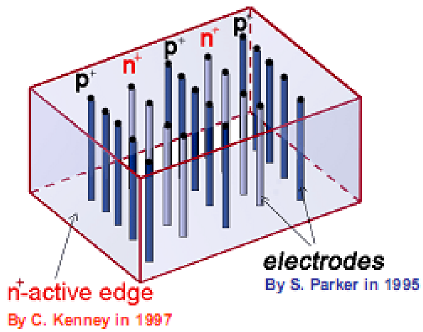

- Electrodes are processed inside the detector bulk instead of being implanted on the wafer's surface (3D silicon detectors - by S. Parker in 1995).
  - I.e. narrow columns along the detector thickness with a diameter of 10µm and separation of 50-100µm.
  - Active Edge Concept : The edge itself is an electrode, thus reducing the dead volume at the edge to <2µm (by C. Kenney in 1997).

3D vs Planar

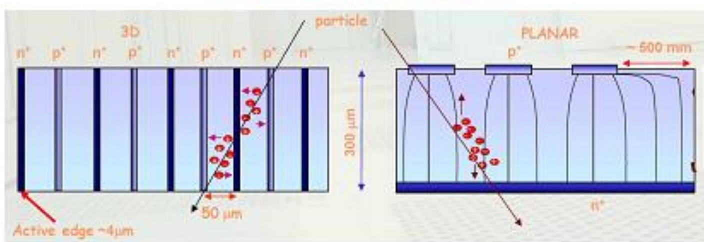

- Almost the same charge generation
- Carrier drift length independent of chip thickness
- Sensitivity up to chip edge
- Lower depletion voltage and noise
- Shorter Drift Length:
  - Increased Radiation Hardness
  - Faster Response
- Higher Capacitance and Increased Production Cost

Basic cross section ~ 1/M^2 so a factor 2x in mass reach is at least a factor 10 x in luminosity – and PDF falloff makes it often very much worse.

Upgrade @ LHC will be a large increase in luminosity. The geometry of vertex detectors will evolve. One option is a 3-d detector.

Vertex Detectors

$$(c\tau)_\tau = 87\ \mu m$$

$$(c\tau)_b \sim 475\ \mu m$$

$$(c\tau)_c \sim (123, 312)\ \mu m \quad (D^o, D^\pm)$$

Pixel size scale set by the lifetimes. PU is a problem so that means occupation of a pixel must be small in order to do robust tracking.

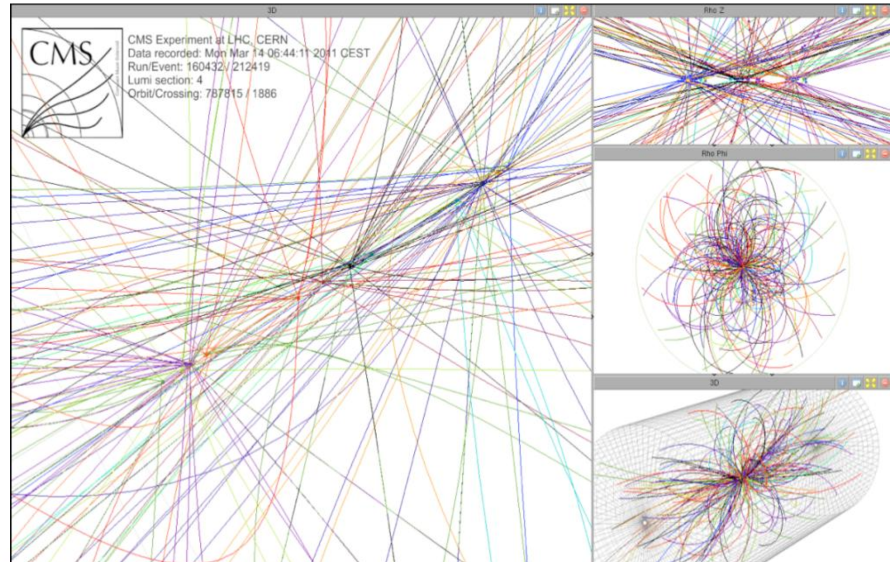

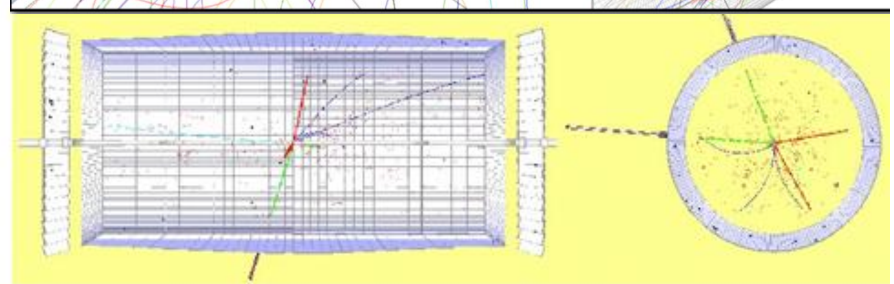

H->Z+Z->e+e+u+u

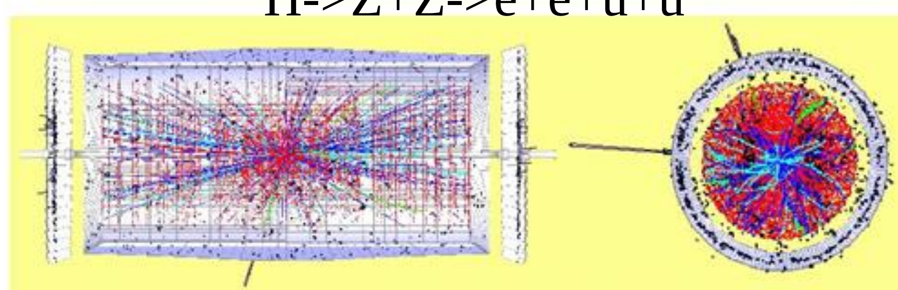

Tracking - Pixels and Strips

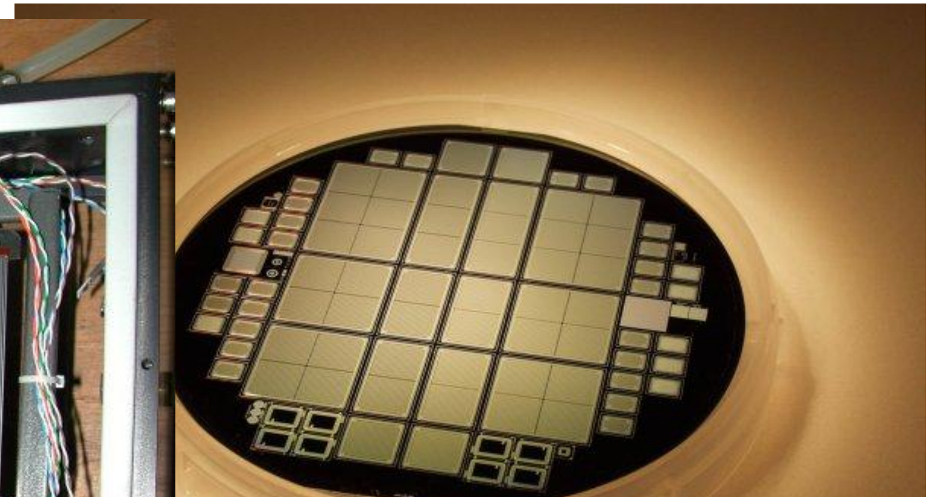

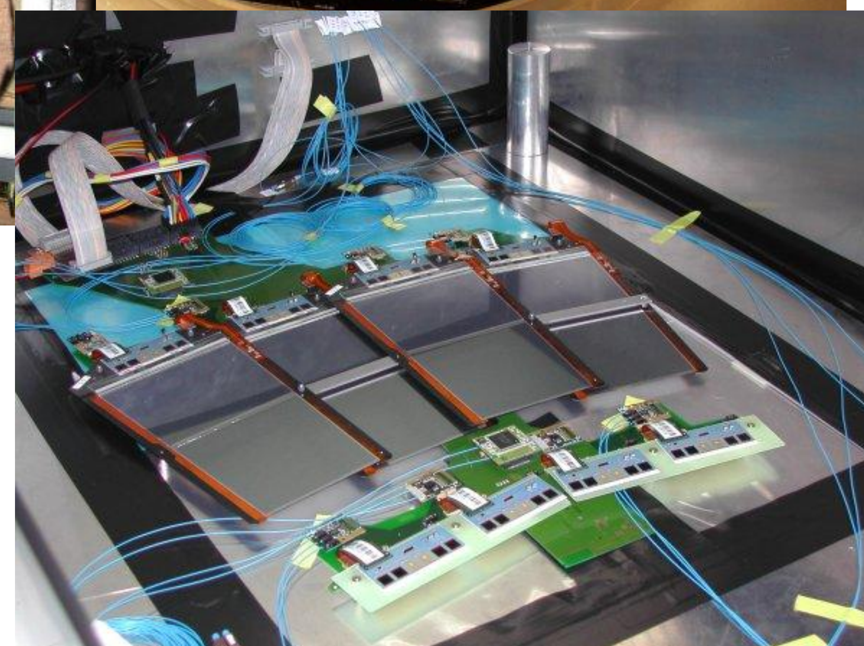

“vertex” pixels ~ 200 um x 200 um. Silicon strips ~ 200 um x 20 cm. For V=50 V, d = 300 um, uE = 42 um/nsec, time~ 7 (21) nsec for e (h). 100 M pixels, |y| < 2.5.

Readout -Noise – Reverse I

High resistivity, back biased Si is ~ a current source.

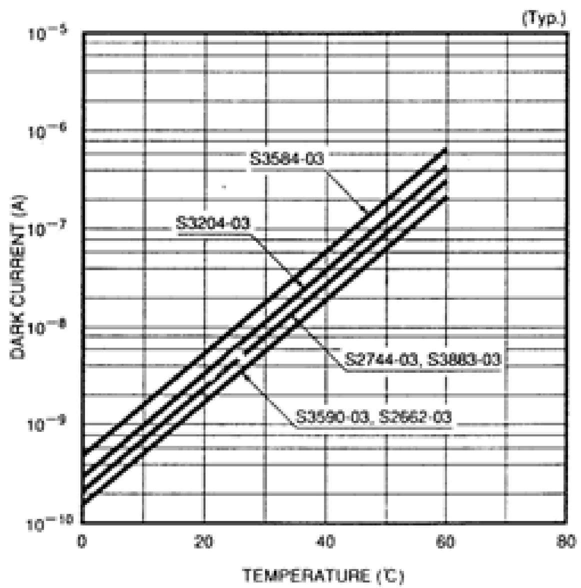

Reverse leakage current as a function of temperature.

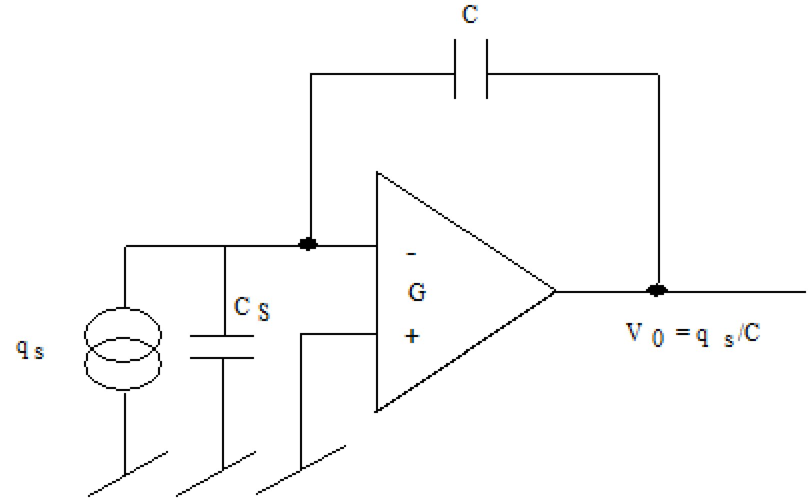

Fig. 9.10: Charge sensitive preamplifier.

The reverse (minority carrier) diode leakage current is a strong (exponential) function of T, exp(qV/kT). The scale is ~ nA. Radiation damage makes defects => impurity states in the diode gap => enhanced leakage current. Run detectors at low T.

Noise – Thermal and Shot

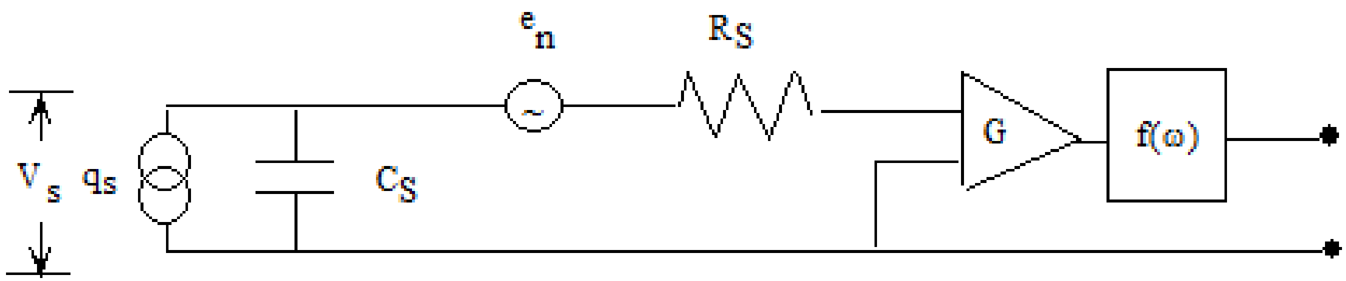

Fig. 9.11: Amplifier and bandwidth limiting filter, f(ω) with source capacity, C_S, source resistance, R_S, source charge, q_S, and input noise voltage, e_n.

Thermal energy kT=> thermal power. Shot noise due to quantized q of I => fluctuations

$$dI_T^2 = \frac{2kT}{R}\left(\frac{d\omega}{\pi}\right)$$

$$dI_s^2 = qI\left(\frac{d\omega}{\pi}\right)$$

$$f(\omega) = G[\omega\tau / 1 + (\omega\tau)^2]$$

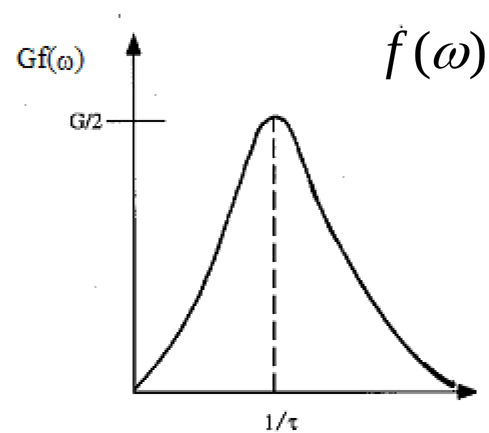

Plot of the transfer function Gf(ω) which → 0 as ω → 0 and as ω → ∞ and peaks at ω = 1/τ.

Must limit the bandwidth to limit the noise - filter

Base Resistance Noise V

$$\sqrt{qI}=0.4nA\sqrt{I(A)\cdot Hz},$$

$$\sqrt{\frac{2kT}{R}}=0.09nA\sqrt{\frac{Hz}{R(\Omega)}}$$

Numerical values for shot and thermal noise

$$R_B = kT/qI_E = 1/g_m,$$

Base current of front end transistor thermal noise

$$d\bar{V}^2 = d\bar{I}_T^2 Z_{CS}^2 + d\bar{I}_S^2 Z_{CS}^2 + d\bar{I}_T^2 R_B^2$$

$$= \left[\frac{2kT}{R_S(\omega C_S)^2} + \frac{qI_B}{(\omega C_S)^2} + \frac{2kT}{g_m}\right]\frac{d\omega}{\pi}$$

rms voltage due to thermal source resistance, base current shot noise and thermal base resistance.

$$<V^2> = \int_{\square}^{\infty} |f(\omega)|^2 \; (d\bar{V}^2/d\omega)d\omega$$

$$= G^2\left[\left(\frac{kT}{2R_S} + \frac{qI_B}{4}\right)\tau/C_S^2 + \frac{kT}{2g_m\tau}\right]$$

Output voltage after the bandwidth limiting filter.

ENC – Series and Parallel

An input charge qs becomes a voltage $V \sim (q_s G / C_S)/e$ at the output at the frequency peak of the filter, $\omega \sim 1/\tau$ in "electron units".

$$(ENC \cdot G / C_s e)^2 \equiv <V^2> \qquad \text{signal}$$

Compare the signal to the Equivalent Noise Charge (ENC) referred to the input.

$$ENCP = (C_S e / G)\sqrt{<V^2>_P} \equiv e\sqrt{\tau\left(\frac{kT}{2Rs} + q\,I_B / 4\right)}$$

$$ENCS = (C_S e / G)\sqrt{<V^2>_S} \equiv e\,C_s\sqrt{kT / 2g_m\tau}$$

The "parallel" noise depends on the shaping time and is due to thermal source resistance and base current shot noise. The "series" noise depends on inverse shaping time, source capacity and thermal base resistance noise.

ENC – Parallel, Series and Shaping

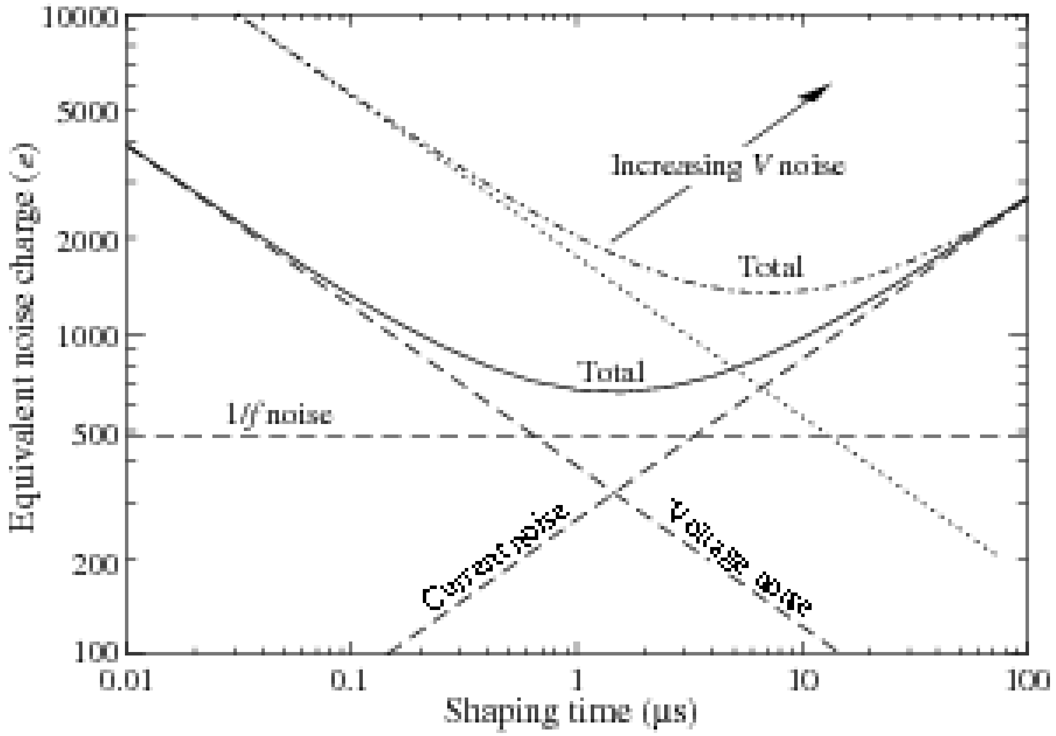

Optimize the shaping time for a particular application. The 2 contributions have different shaping time dependence.

ENC vs Input Capacity

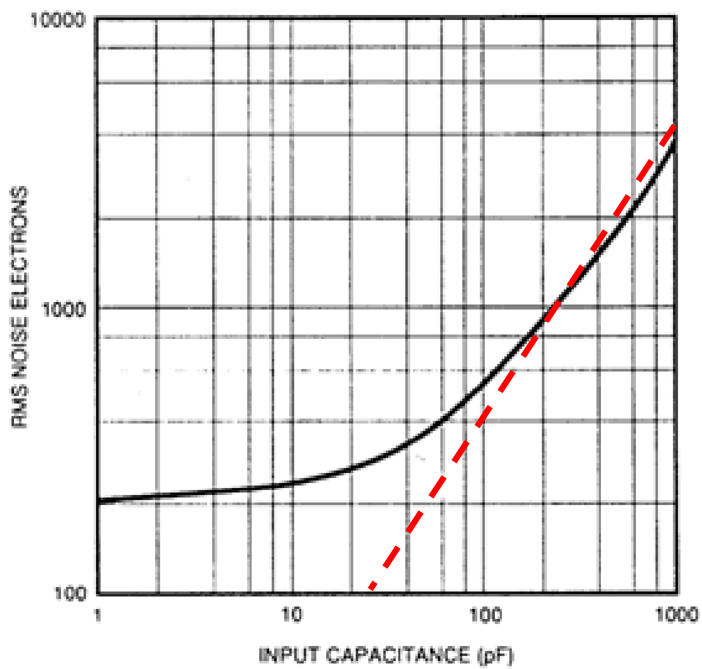

Best Operation

- **Low T**
- **Large Rs (current source)**
- **Small base current**
- **Small source capacity**
- **Small base resistance**
- **Short shaping time (HEP)**
- **Good front end transistor**

Noise in RMS electrons referred to the input as a function of source capacitance for typical preamplifier parameters. The linear dependence for series noise dominance is evident for >100 pF capacity. (From Ref. 12, with permission.)

ENC vs. Shaping Time and Total ENC

Noise from front end transistor

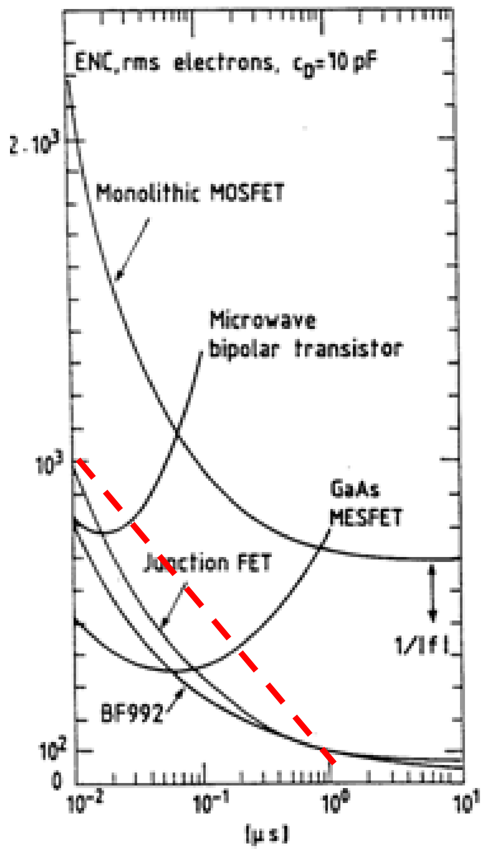

Example:

Source charge = 5.1 fC

$$kT = 300K^o$$

$$g_m = (25\Omega)^{-1}, C_S = 30\,pF, \tau = 10n\sec$$

$$ENC_S = 1125e$$

$$R_S = 1M\Omega,, I_{B=1mA}$$

$$ENC_P = 825e$$

$$S/N = q_s / \sqrt{ENCS^2 + ENCP^2} \sim 23$$

$$Front\ end\ noise = (e_n C_s)/\sqrt{\tau} \sim 800e$$

Equivalent noise charge in RMS electrons as a function of shaping time τ for a 10 pF source capacity and a variety of front end transistors. (From Ref. 13, with

$$(ENCS) \sim e_n C_s / \sqrt{\tau}, e_n \sim 1nV / \sqrt{Hz}$$

Demo – Radioactive Decay

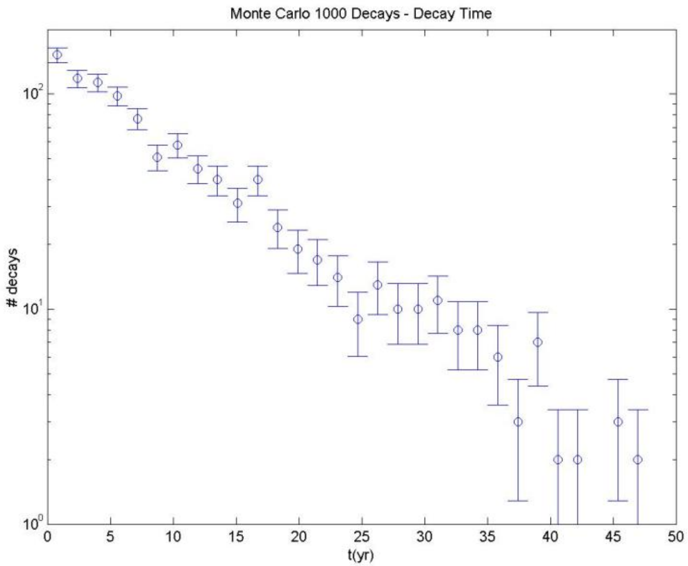

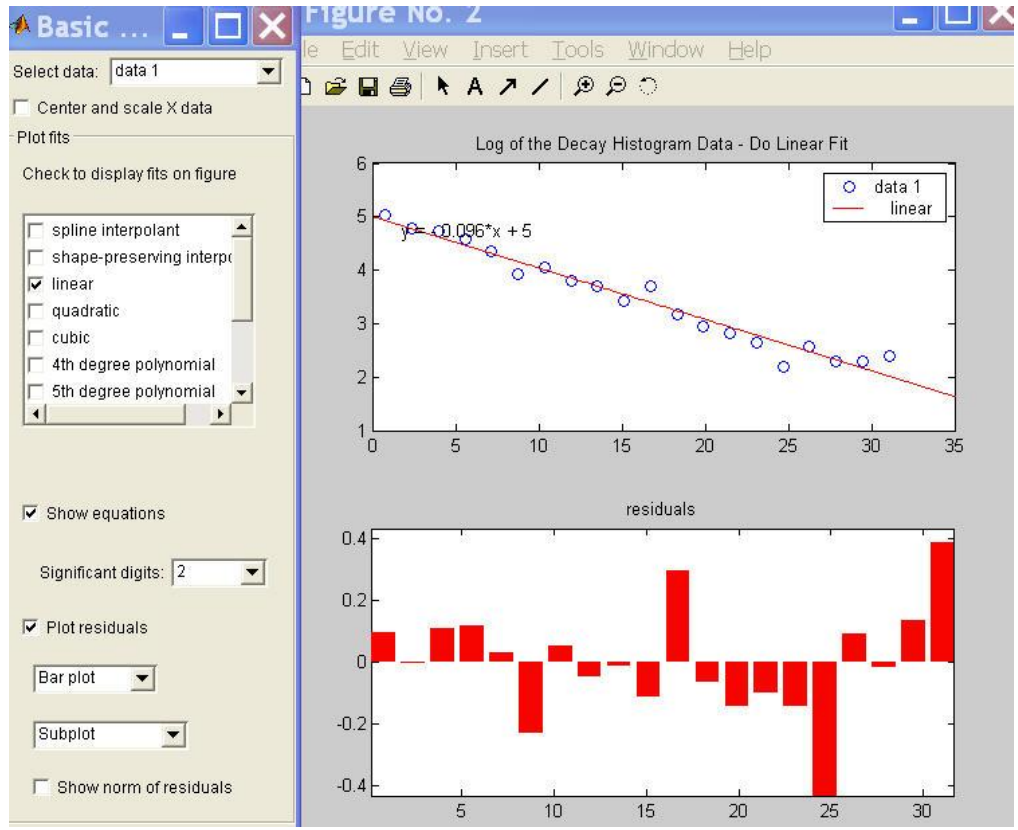

10 year lifetime

Data fitting – with constant errors, using a MATLAB utility.

NR Dipole Radiation

Translate electrostatic results to NR radiative solutions using the addition of a factor = dimensionless quantity – acceleration causes radiation.

$$E \sim \frac{q\sin\theta}{r^2}\left[\frac{ar}{c^2}\right]$$

$$u \sim E^2 \sim \left(qa\sin\theta / rc^2\right)^2 = energy\, density,$$

$$\underline{P} \sim cr^2 E^2$$

$$d\underline{P} / d\Omega = \frac{1}{4\pi}\frac{\left(qa\sin\theta\right)^2}{c^3}$$

$$\underline{P} = \frac{2}{3}\left(qa\right)^2 / c^3$$

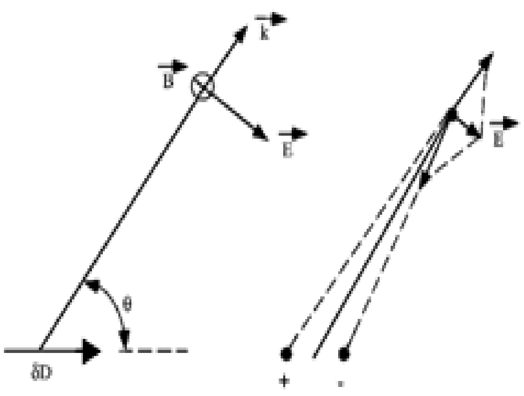

Vector diagram in the far zone for plane waves, $(\vec{E}, \vec{B}, \vec{k})$, caused by dipole acceleration. Static situation shown for comparison

Power through a sphere is independent of r => radiative solution. Power is ~ square of acceleration.

Dipole Power

$$b \rightarrow d, \; dipole \;\; moment = D = 2q[b + d \;\; \sin \omega t]$$

$$\int \sin^2 \theta d\Omega \sim 1/3(8\pi)$$

$$\langle \underline{P} \rangle \rightarrow \left[q^2 d^2 \omega^4 / c^3 \right]$$

$$\langle \underline{P} \rangle = \omega^4 \left(\delta D \right)^2 / 3c^3,$$

$$= \left\langle \ddot{D} \right\rangle^2 / 3c^3, \ddot{D} \equiv \partial D / \partial t^2$$

Relate the acceleration to the size of the radiating system and the frequency.

Result is that power * c^3 is = dipole moment acceleration squared

Thompson Scattering

$$\vec{S} = \frac{c}{4\pi}\left(\vec{E}\times\vec{B}\right), (CGS)$$

Poynting vector

$$\left\langle\left|\vec{S}\right|\right\rangle = \frac{c}{8\pi}\left|E_o\right|^2$$

$$\frac{d\underline{P}}{d\Omega} = \frac{e^2}{4\pi c^3}\left|a\right|^2 \sin^2\theta$$

Dipole radiation

$$a = eE_o / m$$

$$\frac{d\sigma_T}{d\Omega} = \left(e^2 / mc^2\right)^2 \sin^2\theta \equiv \left\langle d\underline{P} / d\Omega\right\rangle / \left\langle\left|\vec{S}\right|\right\rangle$$

$$\sigma_T = \frac{8\pi}{3}(\alpha\bar{\lambda})^2$$

Scattering viewed as the radiation of incoming power

$$\sigma_T = \frac{8}{3}\left[\pi a_0^2\right]\alpha^4$$

$$a_o = \bar{\lambda} / \alpha \; (Section\ I)$$

$$\sigma_T / \pi a_0^2 \sim \alpha^4 \sim 10^{-8}$$

Cross section is Compton wavelength squared times fine structure constant squared. Much smaller the atomic cross section

Thompson Form Factor

$$u \equiv Rr, R = \text{radial wave function}, \psi \sim RY_\ell^m$$

$$\frac{d^2u}{dr^2} + \left[k^2 - U(r) - \frac{\ell(\ell+1)}{r^2}\right]u = 0$$

Scattering off an object with internal structure.

$$u\big|_{r \to o} \to r^{\ell+1}$$

Wave function near r=0 is defined by centrifugal potential

$$\delta_\ell \sim (ka)^{2\ell+1}$$

$$\delta_o \sim -ka >> \delta_\ell$$

Phase shift goes as a power of ka, if ka < 1 S wave dominates

$$\sigma \sim \frac{4\pi}{k^2}\sin^2\delta_o$$

$$\sigma \sim 4\pi a^2$$

Structure has a characteristic size ~ a. Black sphere in this case, totally absorb r<a.

Form Factor - II

$$k^2 + U_o = K^2 \; (interior\ solution\ K)$$

$$tan\delta_o = -ka\left[1 - \frac{\tan(Ka)}{Ka}\right] \sim -ka\left[\frac{(Ka)^2}{3}\right]$$

$$\sigma \to 4\pi a^2\left[(ka)^2/3\right]^2, K \sim k$$

$$\sigma_{RA} \sim a^6/\lambda^4 \sim a^2(a/\lambda)^4, \sigma_{RA}/\pi a^2 \sim (a/\lambda)^4 \sim (ka)^4$$

Wave number For square well

Phase shift, S wave

Small Uo approximation. “Form factor: due to structure of scattering objects.

Why is the sky blue ? Scattering of the blue while transmitting the yellow wavelengths. Rayleigh scattering.

Compton Scattering

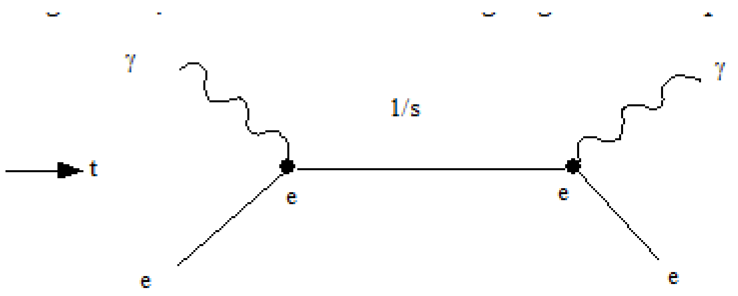

$$\sigma_{KN} \sim \frac{3}{8}\sigma_T\left(\frac{m}{\sqrt{s}}\right)^2[1+ln(\ )] \sim \alpha^2/s$$

SR Thompson/Compton Scattering

$$\sigma_{ee} = \frac{4\pi\alpha^2}{3s} = \frac{87\,nb}{[s(GeV^2)]},\ 1nb = 10^{-33}\,cm^2$$

UR scattering of e - e

In Thompson scattering the radiation emitted has the same frequency as the incident wavelength.

However, as the photon wavelength -> the e Compton wavelength, the emitted photons have a lower energy as the recoil e take off substantial energy.

The cross section then fall with energy, in a fashion clear from the Feynman diagram.

Compton – II, Kinematics

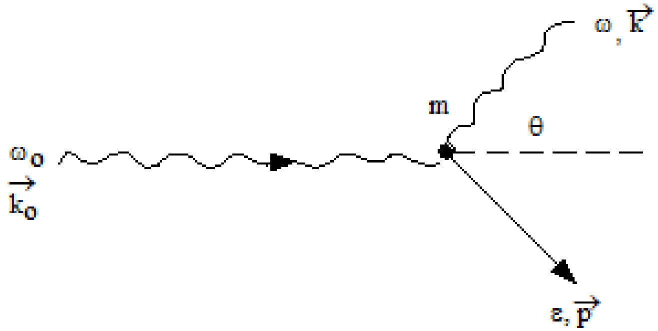

Kinematic definitions for photon scattering off a particle of mass (m).

$$\omega_o + m = \varepsilon + \omega$$

$$\vec{k}_o = \vec{p} + \vec{k}$$

SR conservation of momentum and energy.

$$\left(\frac{1}{\omega} - \frac{1}{\omega_o}\right) = \frac{1}{m}\left(1 - \cos\theta\right)$$

$$\lambda - \lambda_o = 2\pi ƛ(1 - \cos\theta)$$

Energy outgoing is < incident energy. The shift in wavelength is ~ the Compton wavelength and angle dependent (no forward shift)

Compton and QM

kinematic limit for back-scattering, $(1/\omega - 1/\omega_o) = 2/m$, is that the maximum e energy, or "Compton edge", is $T_{max} = \varepsilon_{max} - m = \omega_o[1-m/(m+2\omega_o)] \rightarrow \omega_o$ if $\omega_o \gg m$.

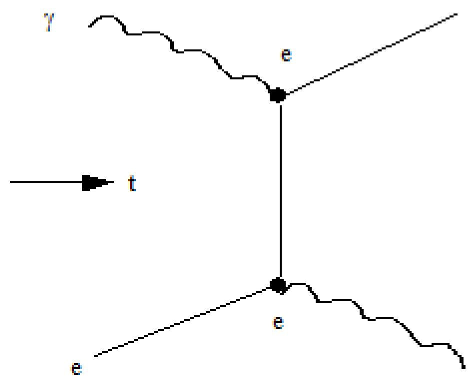

Feynman diagram for Compton scattering. Fermion exchange leads to fast, forward electrons.

The dynamics (t channel exchange) leads to large energy transfer to the e.

$$p^* \sim \sqrt{s}/2 \sim \sqrt{\omega_o m/2},\ d\Omega = d\Omega^*(p^*/p)^2 \sim d\Omega^*\left(\frac{\omega_o m}{2\omega^2}\right)$$

Transform from CM to lab frames. SR "searchlight throws everything forward.

Demo – Angular Distribution

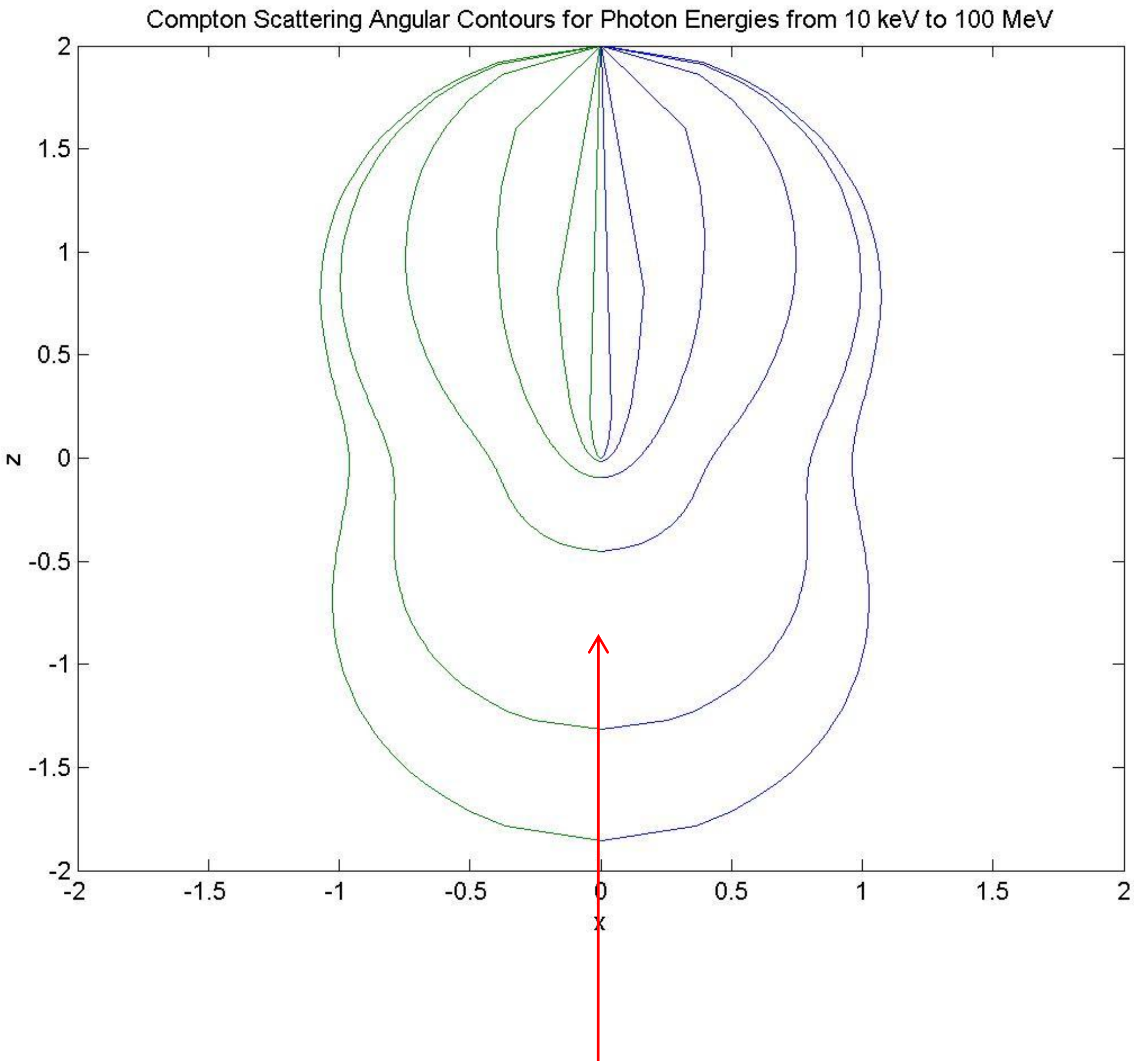

Low energy is ~ forward/backward symmetric. At high incident energy, the final state particles are thrown forward.

Special Relativity

$$x^\mu = (\vec{x}, ct)$$

$$U^\mu = dx^\mu / d(s/c)$$
$$= \gamma(\vec{v}, c)$$

$$ds^2 = dx_\mu dx^\mu = dx^2 - (cdt)^2 = (cdt/\gamma)^2$$
$$\gamma = 1/\sqrt{1-\beta^2}, \ \vec{\beta} = \vec{v}/c$$

$$p^\mu = mU^\mu = (\vec{p}, \varepsilon / c)$$
$$= \gamma m(\vec{v}, c), \vec{v} = d\vec{x}/dt$$
$$\varepsilon = \gamma mc^2$$
$$\vec{p} = \gamma\vec{\beta}mc = \vec{\beta}\varepsilon / c$$

Formulated as 4 dimensional tensorial objects – position, velocity, momentum.

Instead of classical mechanics and time as a label, now need a relativistic invariant – proper time ds.

Momentum and energy are conserved – not kinematic energy due to the rest energy.

Demonstration – Time Dilation

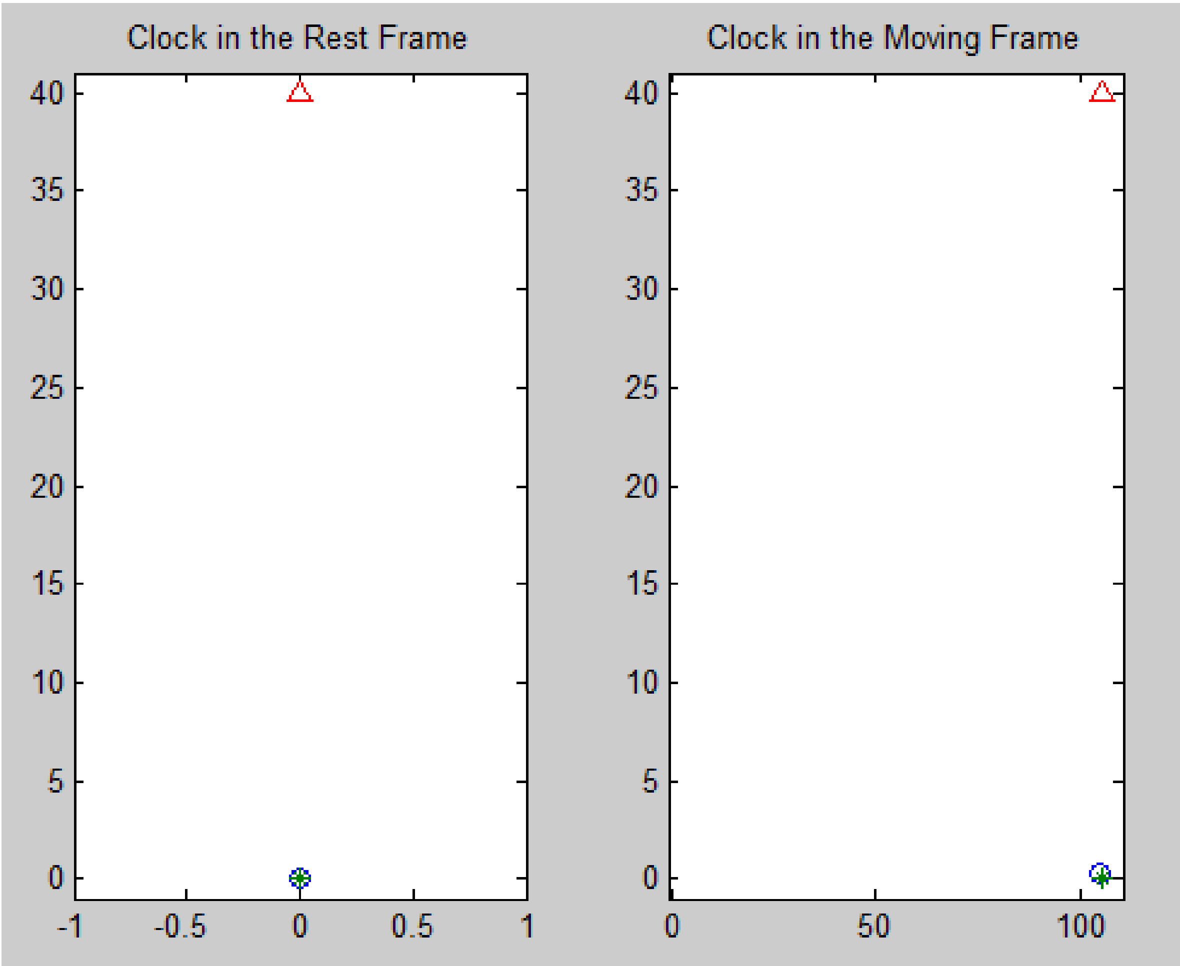

Tick/Tock – in rest frame time is measured on a single clock – proper time. In the moving frame the time is measured on spatially separated, synchronized, clocks. Basically, the length the light travels is just longer.

Acceleration in SR

$$A^{\mu} = dU^{\mu} / d(s/c),$$
$$= \gamma \frac{d}{dt}[\gamma(\vec{v}, c)]$$
$$\frac{d\gamma}{dt} = \gamma^3(\vec{\beta}\cdot\vec{a}), \ \ \vec{a} = d\vec{v}/dt$$
$$A^{\mu} = \gamma^3[\vec{a} + \gamma^2\vec{\beta}(\vec{\beta}\cdot\vec{a}), \gamma^2(\vec{\beta}\cdot\vec{a})]$$

Acceleration in SR is a complex object when formulated in terms of local clocks and rulers.

In SR acceleration is the proper time rate of change of the 4-velocity.

$$\underline{P} = \frac{2}{3}\frac{e^2}{c^3}A_{\mu}A^{\mu}$$
$$= \frac{2}{3}(e^2/c^3)\gamma^6\left[\left|\vec{a}\right|^2 - \left|\vec{\beta} \text{ x } \vec{a}\right|^2\right]$$

The SR power radiated by a charge due to acceleration is the "length" of the 4-acceleration.

Radiation in Linear/Circular Acceleration

$$\left(\underline{P}\right)_{o} = \frac{2}{3}\frac{e^{2}}{c^{3}}\gamma^{4}\left|\vec{a}\right|^{2}$$

The power radiated in circular motion is much larger than expected in NR case. Note – that is why e accelerators are linear recently.

$$A_{\mu} = \left(\frac{\gamma\beta}{m}\right)\frac{d}{dx}\left[\varepsilon\left(\vec{\beta},1\right)\right], dx = \beta c dt$$

$$\left(\underline{P}\right)_{LIN} = \frac{2}{3}\frac{e^{2}}{m^{2}c^{3}}\left(\frac{d\varepsilon}{dx}\right)^{2}$$

$$\left(\underline{P}\right)_{LIN} = 2/3\,(e^{2}/c^{3})\left|\vec{a}\right|^{2}\gamma^{6}$$

In the linear case, the required power is simply proportional to the lab energy supplied per unit length – e.g. r.f. cavities.

Searchlight Effect

$$\varepsilon = \gamma(\varepsilon^* - \beta p^* \cos\theta^*) = \gamma\varepsilon^*(1-\beta\cos\theta^*)$$

$$\frac{1}{\gamma^2} = 1-\beta^2$$

$$\beta \equiv 1-\delta\beta$$

$$\beta^2 \cong 1-2\delta\beta$$

$$\frac{1}{\gamma^2} \cong 2\delta\beta$$

$$\cong 2(1-\beta)$$

$$1-\beta\cos\theta \sim 1-\beta(1-\theta^2/2)$$

$$\sim \frac{1}{2}\left(\frac{1}{\gamma^2}+\theta^2\right)$$

$$\langle\theta\rangle \sim 1/\gamma$$

Transform the energy of the radiation from the C.M> (starred) frame to the lab observer frame.

For a more isotropic distribution in the C.M, the radiation in the lab frame is typically localized in a small angle region. This is called the searchlight effect.

Demo - Radiation

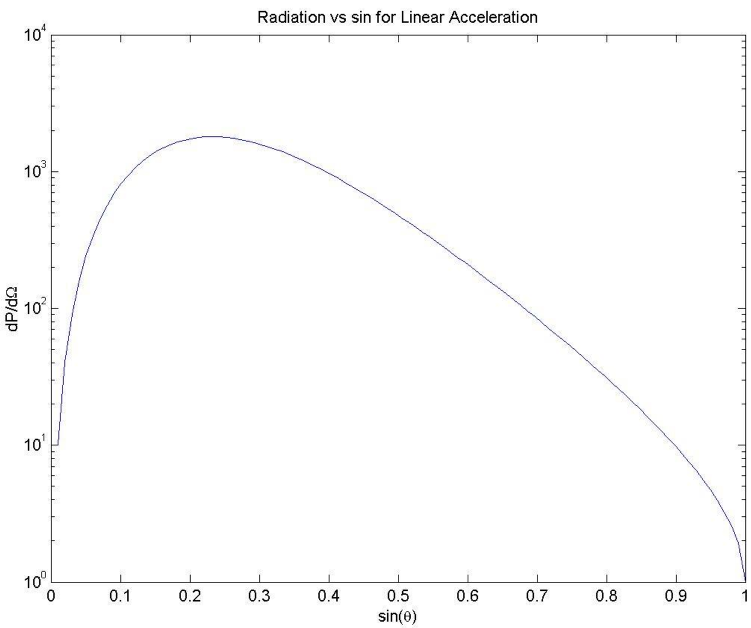

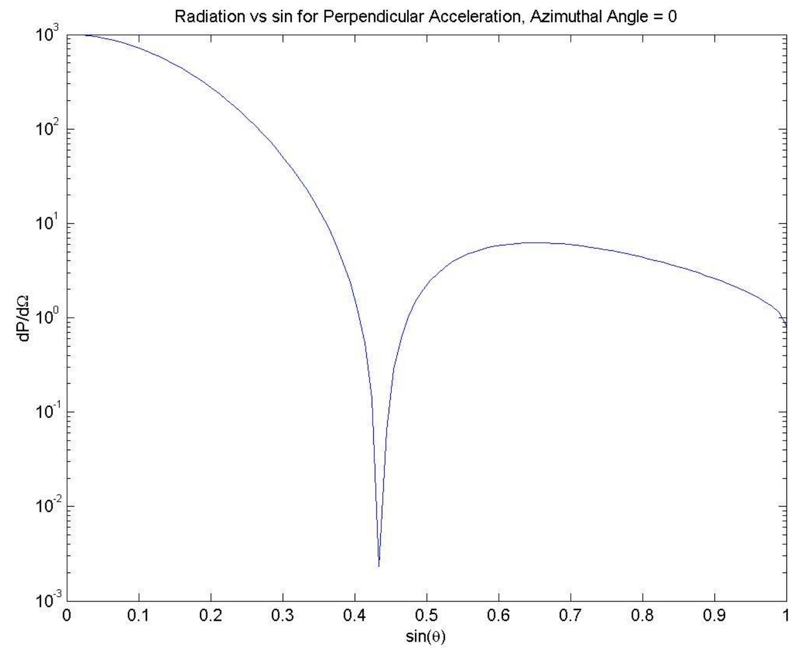

linear

$$d\underline{P}_{LIN} / d\Omega = \alpha a^2 / 4\pi c^3 \left[\sin^2\theta / (1-\beta\cos\theta)^5\right]$$

$$d\underline{P}_{LIN} / d\Omega \to \alpha a^2 / 4\pi c^3 (\sin^2\theta)$$

circular

NR dipole radiation goes forward in both the linear and circular case.

Demo – "Searchlight"

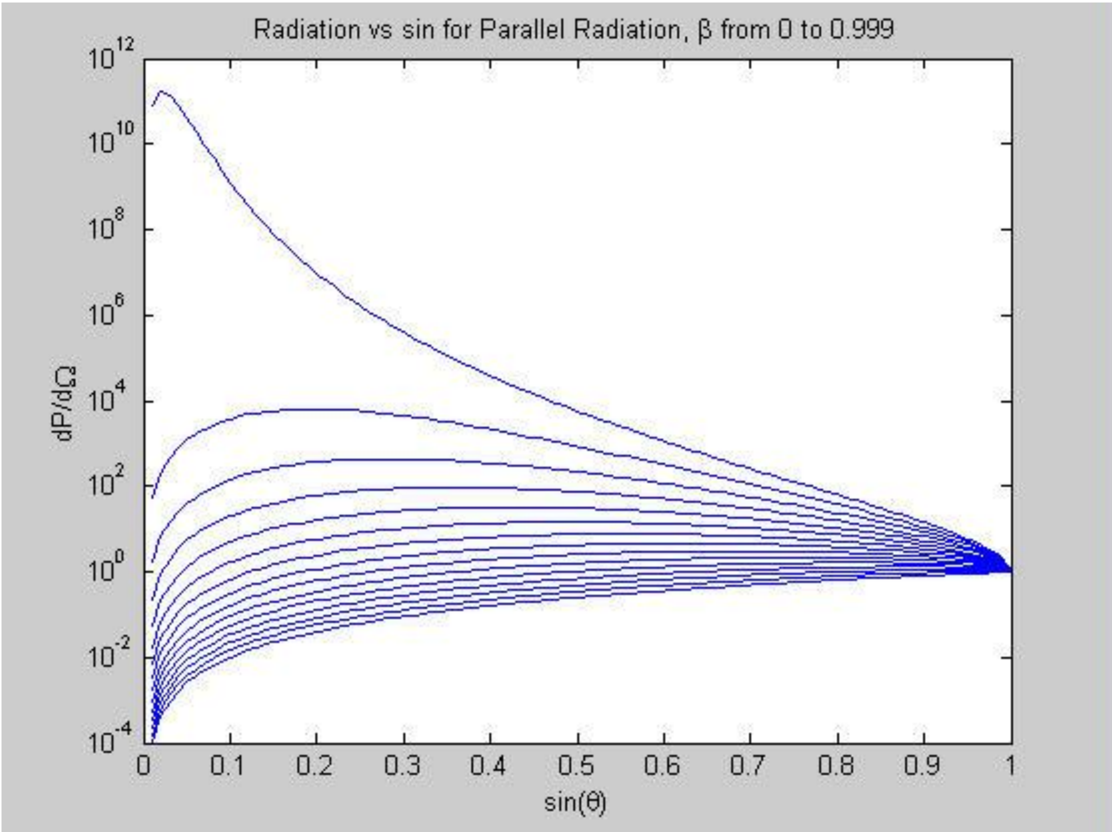


```
 Radiation of Accelerated Charge Moving Relativistically
Enter the Instantaneous Speed of the Charge w.r.t. c: 0.9
The Radiation Field is Plotted w.r.t the Angle Between the Observer and the Acceleration
Linear Radiation Radiates gamma^4 Less than Circular Acceleration
For Perpendicular Radiation the Polar Angle is between the Velocity(z) and the Observer
For Perpendicular Radiation the x Axis is the Direction of the Acceleration
```

The sharp rise of the total radiated power with energy is very evident, as is the forward nature of the angular distribution.

Circular Acceleration

$$\omega_o \sim c\beta / a$$

$$\omega_c \sim \gamma^3 \omega_o$$

$$\equiv 3\gamma^3 c / 2a$$

$$\Delta \mathrm{E} = \left(\frac{2\pi a}{c\beta}\right)\underline{P}$$

$$\sim \left(\frac{4\pi}{3}\alpha\gamma\right)\left(\gamma^3\omega_o\right) \sim\sim \gamma^4$$

$$\sim \alpha\gamma\omega_C$$

$$\sim \left[dI(\omega)/d\omega\right]\left[\Delta\omega = \omega_c\right]$$

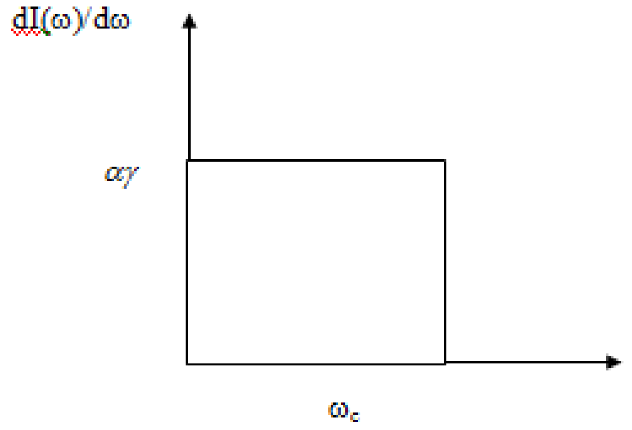

Schematic representation of the frequency distribution of the intensity for circular motion.

The NR frequency is given by the velocity and the radius. The SR frequency (time dilation) rises rapidly with energy and extends up to a critical frequency. The energy loss due to radiation is the power times the lab time interval. This leads to the fourth power. The frequency spectrum is ~ flat out to the critical frequency.

Synchrotron Radiation

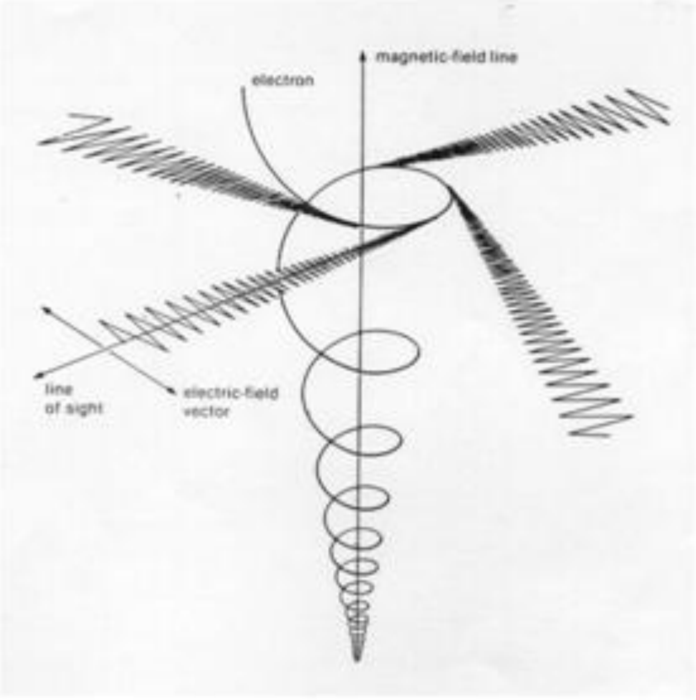

Schematic representation of the emission of synchrotron radiation by an electron spiraling in a magnetic field.

An e in a magnetic field spirals around the field line while emitted synchrotron radiation => smaller radius of curvature – the “death spiral”.

$$\Delta E(keV) = 90[E(GeV)]^4 / a(m)$$

$$\hbar\omega_c(keV) = 2.2\left[E\left(GeV\right)\right]^3 / a(m)$$

Numerical values for e at bend radius a.

Demo – Circular, SR

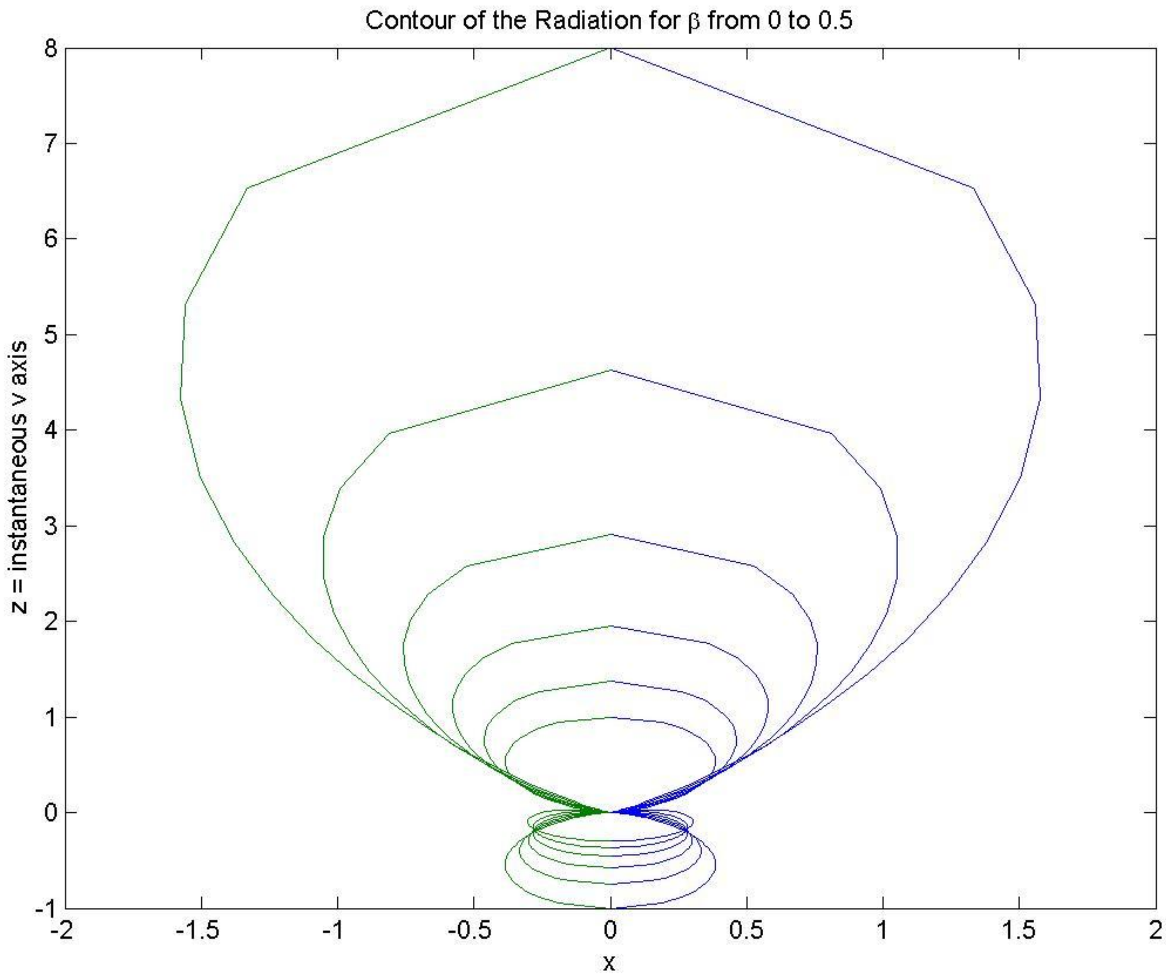

As before, the dipole like pattern become much larger in absolute power radiated and become much more forward peaked.

Pair Production

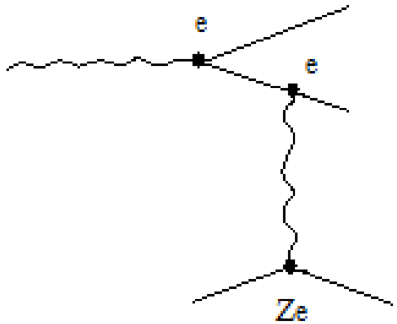

Feynman diagram for photon pair production in the field of a nucleus with atomic number Z.

An isolated charged particle cannot radiate (good idea or we would not exist). A photon can virtually decay into an electron-positron pair by using energy from the photons in the Coulomb field of a nucleus.

As the Compton scattering cross section falls off with photon energy, the pair production becomes the dominant energy loss mechanism for photons at high energies.

Pair Production - II

$$\sigma_{pair} = \frac{7}{9}\sigma_B$$

$$\sigma_B \sim \left(Z^2\alpha\right)(\alpha ƛ_e)^2\,[\ln(\,)]$$

$$\frac{\left(d\sigma_{pair}/dy\right)}{d\sigma_B/dy} \sim \frac{\alpha/\pi(1/y^3)}{(1/y)}$$

$$y \cong E_\gamma / E$$

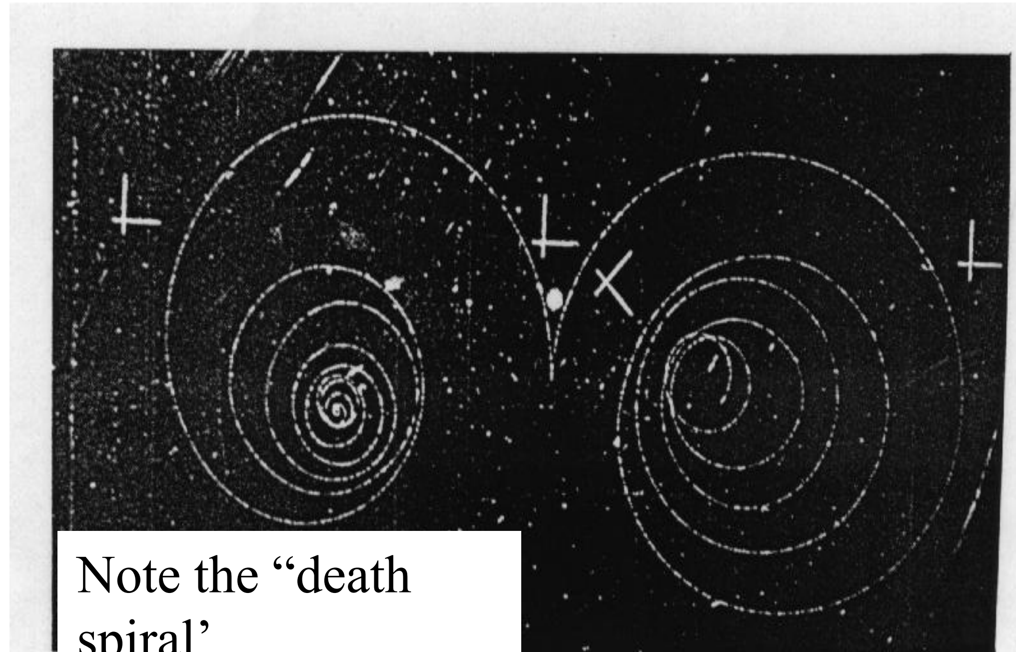

Note the "death spiral'

Pair production and Bremmstrahlung are closely related processes (later). They are coherent over the small size of the nucleus and go like the third power of the fine structure constant – see Feynman diagram. Pair production favors soft electrons.

Bremm – WW Virtual Quanta

$$dU = \int du = \iint E(\omega)^2 \, d\omega 2\pi b db$$
$$= \int [dU / d\omega] d\omega$$

$$dU / d\omega = 4\alpha / \beta^2 \left[\ln(\ \ ) \right]$$

$$dU = \hbar \omega dN_\gamma$$

$$\frac{dN_\gamma(\omega)}{d\omega} \sim \frac{\alpha}{\beta^2}\left(\frac{1}{\omega}\right)[\ln(\,)]$$
$$= \frac{2\alpha}{\pi}\left(\frac{1}{\beta^2}\right)\left(\frac{1}{\omega}\right)[\ln(\,)]$$

The nucleus can be viewed as a source of virtual photons which then scatter incoming charged particles. Recall that a Coulomb collision has energy loss ~ the inverse of the velocity squared.

The energy can be converted from energy and frequency to the number of virtual photons of a given frequency. The basic dependence of the spectrum is that it falls as the inverse of the photon energy.

Bremm - II

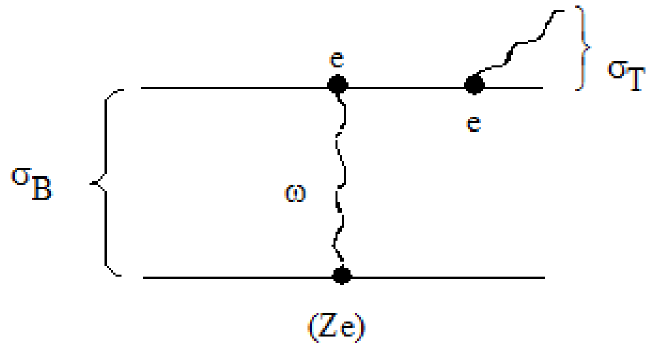

The Feynman diagram is closely related to that for photon pair production. The nuclear Coulomb field supplies the virtual photon which allows the electron to radiate a photon and still conserve energy/momentum.

: Feynman diagram for Bremsstrahlung in the field of a nucleus of atomic number Z.

$$\frac{d\sigma_B}{d\omega} \sim Z^2 \frac{dN_\gamma}{d\omega}\sigma_T$$ coherent

$$\frac{d\sigma_B}{d\omega} \sim \frac{\left(Z^2\alpha\right)}{\omega}\left(\alpha \bar{\lambda}_e\right)^2 [\ln(\,)]$$

$$dE \sim \int_o^E (\hbar\omega)\left(\frac{N_o \rho dx}{A}\right)\left(\frac{d\sigma_B}{d\omega}\right) d\omega$$

The Bremm frequency spectrum can be (NR) viewed as the Thompson scattering of the soft, virtual photons of the nucleus. The energy loss of the electrons has a characteristic inverse photon energy emission spectrum.

Radiation Length

Xo(gm/cm^2) = [180(A/Z)]/Z.

$$\frac{1}{E}\left(\frac{dE}{\rho dx}\right) \equiv \frac{1}{X_o}, E(x) = E(o)e^{-\rho x/X_o}$$

$$X_o^{-1} = \frac{16}{3}\left(\frac{N_o}{A}\right)(Z^2\alpha)(\alpha \lambda\!\!\!^{-}_e)^2[\ln(\,)]$$

$$\sim (Z/A)Z \sim Z$$

$$\sigma_B \equiv [A/(N_o \rho X_o)]$$

$$X_o = \langle L \rangle$$

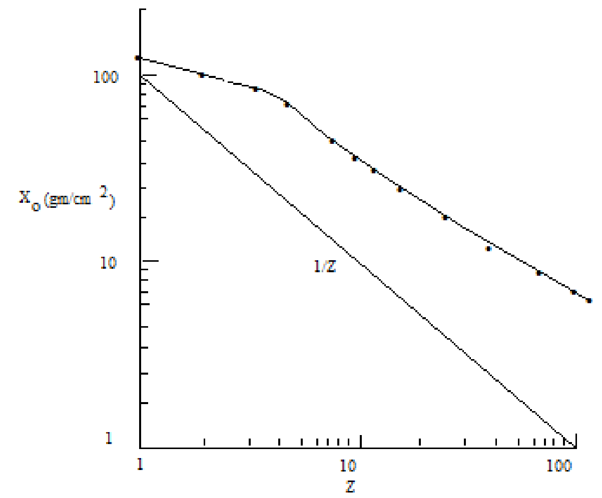

Plot of the radiation length X_0 in gm/cm^2 as a function of the atomic number Z. The line, ____, has the functionality 1/Z for comparison.

In Lecture I the radiation length appeared – arbitrarily. Here it is defined to be the mean free path to emit a photon. It goes as Z (coherence less 1/A) times the third power of alpha (counting vertices).

Muon Energy Loss

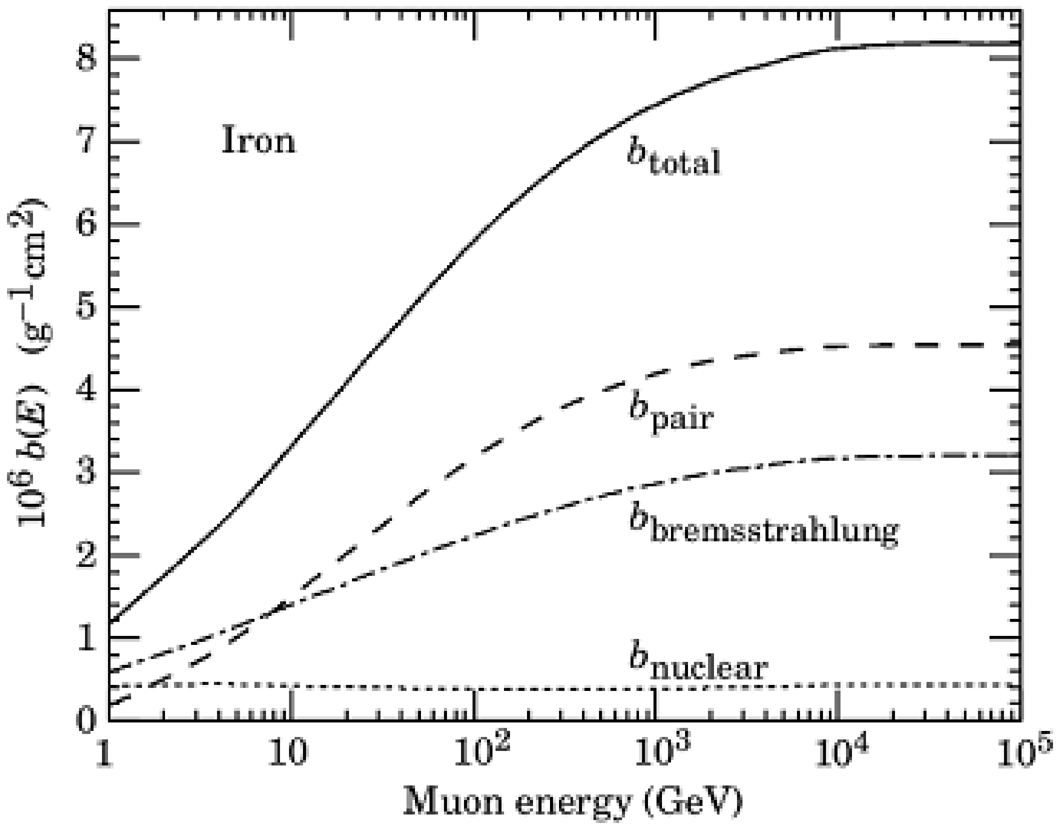

$$E_{c\mu} / E_{ce} \sim (m_\mu / m_e)^2$$

If the critical energy was ~ 10 MeV for e, then the critical energy for muons will be ~ 420 GeV. That becomes important at new colliders such as the LHC

Muons are just heavy electrons (so far), responding to the same forces as electrons. That means the muon energy loss is dominated by radiative processes at high energies.

Tracker Material

beam pipe, pixels, strips

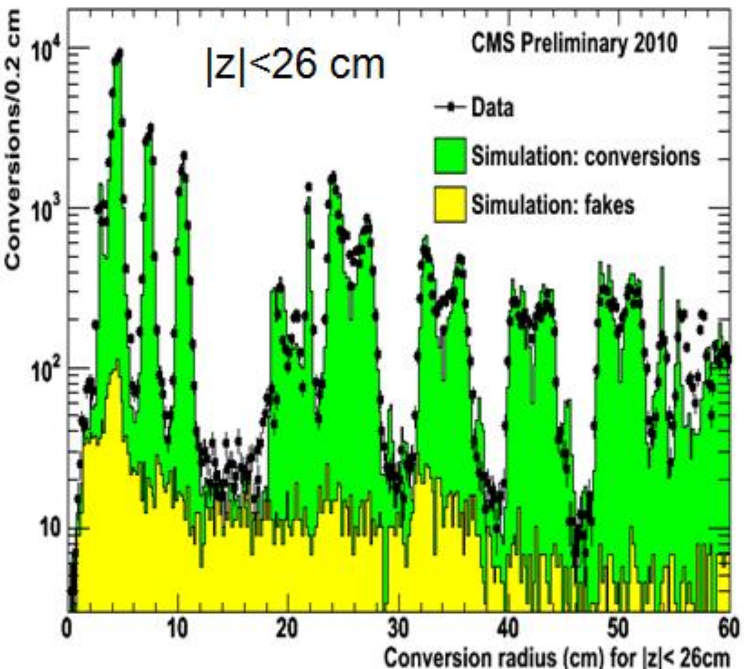

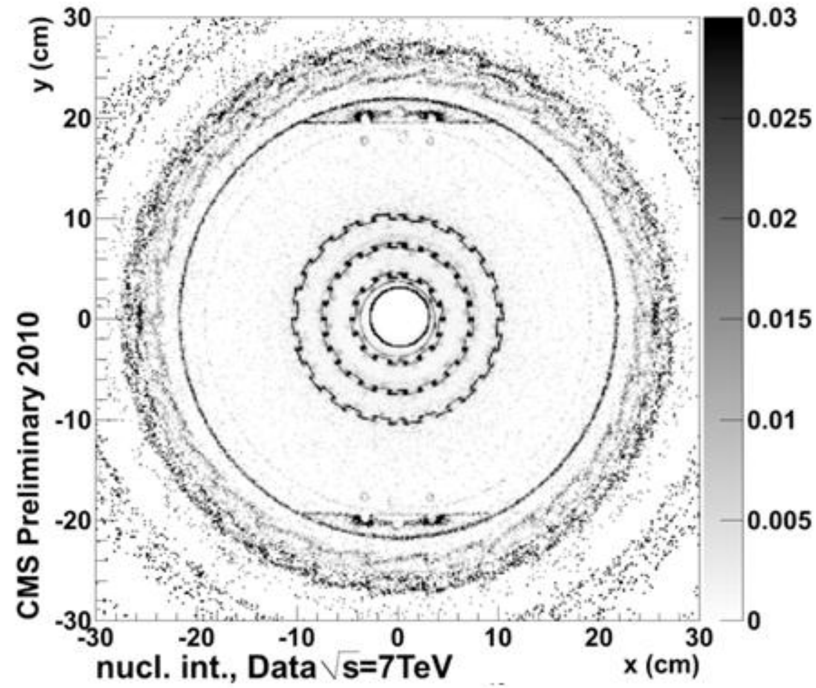

radius

For a complete understanding of the momentum scale and resolution a detailed understanding of the tracker material throughout the system is needed – use photon conversions for high Z and nuclear interactions for low Z material.

Particle ID

$$\sigma_N \sim A^{2/3} \lambdabar_p^2$$

$$\sigma_B \sim (Z\alpha)^2 \alpha \lambdabar_e^2$$

$$\lambda_1 / X_o \sim (Z/A)/[5.1A^{2/3}]$$

It is interesting to note that the nuclear cross section, as we saw in Section 1, goes as $A^{2/3}$ times the Compton wavelength of the proton squared. By comparison, the Bremsstrahlung cross section goes as Z^2 because of coherence. Since this is an electromagnetic process with 3 vertices, (Fig. 10.13), we pay the penalty of a factor α^3. Even so, the electromagnetic Bremsstrahlung cross section is comparable to the nuclear cross section for A~3 (lithium). A glance at Table 1.2 shows that for Be and heavier elements the characteristic length for radiation, $(X_o)_{Be} = 65.2\ \mathrm{gm/cm^2}$ is less than the characteristic length for nuclear interaction, $(\lambda_1)_{Be} = 75.2\ \mathrm{gm/cm^2}$. It is amusing that this particular electromagnetic process is stronger than the "strong" interaction because of coherence effects. We will explain how the fact that $X_o >> \lambda_I$ for heavy elements is exploited to provide calorimetric "particle identification" in